Low-Complexity Velocity Estimation in High-Speed Optical Doppler Tomography Systems

Milos Milosevic, Wade Schwartzkopf, Thomas E. Milner, Brian L. Evans, and Alan C. Bovik

Department of Electrical and Computer Engineering
The University of Texas at Austin, Austin, TX 78712-1084

{milos,wade,milner,bevans,bovik}@ece.utexas.edu

Abstract – *Optical Doppler Tomography (ODT) is a non-invasive 3-D optical interferometric imaging technique that measures static and dynamic structures in a sample. To obtain the dynamic structure, e.g. blood flowing in tissue, a velocity estimation algorithm detects the Doppler shift in the received interference fringe data with respect to the carrier frequency. Previous velocity estimation algorithms use conventional Fourier magnitude techniques that do not provide sufficient frequency resolution in fast ODT systems because of the high data acquisition rates and hence short time series. In this paper, we propose a nonlinear algorithm that uses the phase shift between two successive scans of interference fringe data to give a high-resolution estimate of the Doppler shift. The algorithm detects Doppler shifts of 0.1 to 3 kHz with respect to a 1 MHz carrier. In processing 5 frames/s with 100 x 100 pixels/frame and 32 samples/pixel, i.e. 1.6 million samples/s, the algorithm requires 26 million multiply-accumulates/s. The algorithm works well at 4 bits/sample. The low complexity and small input data size are well-suited for real-time implementation in software. We provide a mathematical analysis of the Doppler shift resolution by modeling the interference fringe data as an AM-FM signal.*

I. Introduction

Optical Doppler tomography (ODT) is a non-invasive optical interferometric imaging technique. ODT systems incorporate laser Doppler flowmetry and optical coherence tomography to produce high-resolution images of static (e.g. fibrous tissue) and dynamic (e.g. flowing blood) structural components in highly scattering samples. ODT systems utilize a Michelson interferometer that has a broadband light source that emits in a single mode to measure light

backscattered from turbid media with high spatial resolution (~10 µm) and sensitivity (dynamic range of 100 dB). High spatial resolution in depth is obtained since only light backscattered from the turbid medium with equal optical path lengths in the sample and reference paths will produce interference fringe data (IFD). The carrier frequency (f_c) of the IFD is established by phase modulation of light in the reference and/or sample paths of the interferometer. The IFD is digitized at each location in the sample by raster scanning light in the sample arm.

Any flow in the tissue that is in line with the source beam will result in backscattered light whose spectrum exhibits a Doppler spread (σ_d^2) and shift (f_d) away from the carrier frequency. Doppler shift is proportional to the velocity of components moving along the incident light direction. ODT has the ability to image biological tissue in three spatial dimensions. Since the lateral movement of the source beam can be precisely controlled to resolution of 2-15 µm, high spatial resolution images can be obtained.

The first Doppler velocimetry system [1] appeared shortly after the invention of the laser in the 1960s. Because sources in early Doppler velocimetry systems had narrow spectral emission profiles, poor control over depth, low image resolution, and slow frame acquisition rates were obtained. In 1995, a novel method of Doppler velocimetry incorporated a broadband light source [2,3] which gave
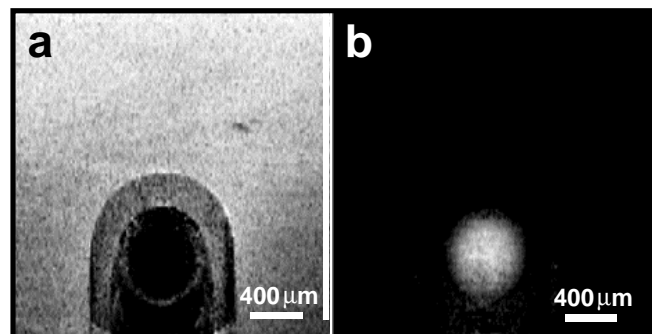

Figure 1: ODT images of polystyrene microspheres in a polyethylene conduit submerged 1 mm below the surface in a turbid sample: (a) ODT structural image of flowing microspheres, and (b) ODT velocity image of flowing microspheres. [3]

better control over depth and higher image resolution and also allowed flow velocity measurements in turbid media. This first ODT system used the amplitude of the received signal for the greyscale value of the pixels in the structural image, while the Doppler shift information is used to calculate the velocity in the image. The Doppler shifts are calculated as the difference between f_c and the centroid of the short-time Fourier transform (STFT) [6] of the IFD obtained at the point being imaged. The calculated Doppler shift is used to create the ODT velocity image. Examples of structural and velocity images are shown in Figure 1.

Current generation ODT systems [2,3,4,5] require several minutes to produce one frame. The next generation systems are targeting 5 frames/s at a resolution of 100×100 pixels per frame. With only 25% of the scanning time spent acquiring data, we have 2.5 µs/pixel of IFD recording time. Doppler shifts in ODT typically range from 0.1 to 3 kHz; shifts below 0.1 kHz are assumed to be insignificant. Over the range of Doppler frequencies, 2.5 µs of IFD recording time implies that we would have less than 0.0075 periods of the Doppler shift. The short time of the acquisition and the noise of the recorded IFD severely limit the resolution of STFT-based algorithms.

In this paper, we present a new velocity estimation for next generation ODT systems that can detect 0.1 to 3 kHz Doppler shifts in a 1 MHz carrier wave using data records of only 1 µs obtained in a noisy environment. To process 5 frames/s, the algorithm requires 26 million multiply-accumulates/s, so it can be implemented in real-time in software. The primary contributions of this paper are:

1. A new low-complexity nonlinear algorithm resolving Doppler shifts on the order of 1 kHz in a 1 MHz carrier wave, and

2. An analysis of the algorithm's resolution based on AM-FM modeling of the interference fringe data.

An AM-FM model appropriately describes the behavior of the IFD, with the constraint that the amplitude and phase modulation functions are smooth. The IFD amplitude defines the structural ODT image of the observed tissue. The phase provides information used to form the ODT velocity image. The rationale for using an AM-FM model is the wealth of knowledge on the subject and the applicability of many published demodulation techniques, such as the energy separation algorithms in [7].

II. Modeling

Figure 2 shows the model of an ODT system. $X(f)$ is the Fourier transform of the source signal; $IFD_n(t)$ is the recorded IFD; $n(t)$ is independent, identically distributed Gaussian noise with zero mean and variance σ^2; f_c is the signal carrier frequency; f_d is the Doppler shift; and f_c+f_d is the mean of the Doppler spread of variance σ_d^2.
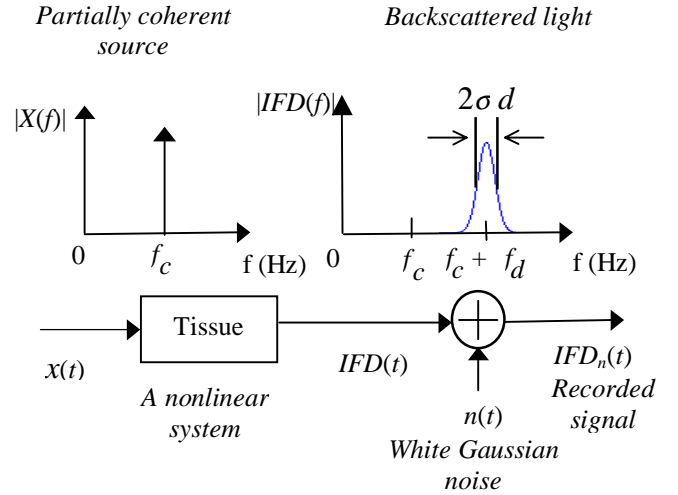

Figure 2: Signal processing in an optical Doppler tomography system.

The model for $IFD_n(t)$ is based on the physics of the light-tissue interaction [8]. Because light incident on the sample is well approximated by a Gaussian beam, scattering from moving constituents (e.g., red blood cells) gives a range of Doppler shifts that are normally distributed about a center frequency, f_d. From the results of Monte Carlo simulations of light scattering in tissue, we write the $IFD_n(t)$ as a superposition of interference fringes due to each incoming light direction in the incident Gaussian beam with amplitude W_i, frequency shift f_i, and a random phase uniformly distributed between zero and 2π: [8]

$$IFD_n(t) = \sum_{i=0}^{\infty} W_i \cos(2\pi f_c t + 2\pi f_i t + \varphi_i) + n(t) \qquad (1)$$

Here, φ_i is the initial phase which is uniformly distributed from 0 to 2π, W_i are samples of a Gaussian-shaped function, and f_i is a frequency shift due to multiple scattering of light in the sample, and the spacing between the successive components in the frequency domain is Δf.

In (1), assuming small Δf and ignoring additive noise,

$$IFD_n(f)u(f) = W(f)\exp[j\xi(f)] * \delta(f - f_c - f_d) \quad (2)$$

where $W_i = W(f)\big|_{f=i\Delta f}$, $\varphi_i = \xi(f)\big|_{f=i\Delta f}$, $u(f)$ is the step function, and $*$ denotes convolution. Since $IFD_n(t)$ is narrowband, it can be described using an AM-FM model:

$$IFD_n(t) \cong A(t)\cos[2\pi(f_c + f_d)\,t + \phi(t)] + n(t) \qquad (3)$$

The AM-FM model is used in speech recognition [7], and image processing [9], among other fields. One of the first references on the subject is by Carson [10].

By ignoring the additive noise term, (3) becomes

$$IFD_n(f)u(f) = \frac{1}{2}[A(f) * \Theta(f)] * \delta(f - f_c - f_d) \qquad (4)$$

where $A(f) = \Im\{A(t)\}$, $\Theta(f) = \Im\{\exp[j\phi(f)]\}$ such that $\Im\{x\}$ denotes the Fourier transform operator on x.

Hence, the models for $IFD_n(t)$ given by (1) and (3) can be tied together using the relationship

$$A(t)\exp[j\phi(t)] = 2w(t) * \Im^{-1}\{\exp[j\xi(f)]\} \qquad (5)$$

where $w(t) = \Im^{-1}\{W(f)\}$ and both the amplitude function $A(t)$ and the phase function $\phi(t)$ are slowly-varying functions compared to $\cos(2\pi f_c t)$. Their bandwidth accounts for the Doppler spread in the interference fringe data. Neither $A(t)$ nor $\phi(t)$ are known when the $IFD_n(t)$ is recorded.

III. Proposed Algorithm

If the structural orientation of the illuminated sample does not change over a short time interval Δt, then $\phi(t) = \phi(t-\Delta t)$. In the case of blood flow,

$$\Delta t_{max} \approx \frac{1}{\text{velocity of blood}} \leq 30\,\text{ms}$$

We use $\Delta t = 1$ ms in this paper.

We correlate of $IFD_n(t)$ and $IFD_n(t-\Delta t)$ to eliminate the unknown initial phase, $\phi(t)$. The cross-correlation

$$R_T(\tau, \Delta t) \propto \cos[2\pi(f_c + f_d)(\tau - \Delta t)] \qquad (6)$$

Within the short time interval Δt, the Doppler shift f_d will cause a phase shift. The location of the peak of the cross-correlation will give the time difference, τ_{max}, between the waves, and thus the phase difference between the two IFD's. If we assume only one cycle of $R_T(\tau, \Delta t)$, then the estimate of f_d is

$$\hat{f}_d = \text{mod}(f_d \Delta t, 1) = \frac{\text{mod}(f_c \Delta t, 1) - f_c \tau_{max}}{\tau_{max} - \Delta t} \qquad (7)$$

where

$$\tau_{max} = \arg\max_{\tau} R_T(\tau, \Delta t).$$

The algorithm does not estimate each particular frequency component present in the $IFD_n(t)$, but instead finds their average, which is exactly the desired Doppler shift assuming a symmetric Fourier spectrum around the carrier frequency f_c. Finding this estimate for every pixel produces an ODT velocity image of the sample.

Equation (7) produces a value for a single pixel. The histogram of the estimates of Doppler shift for 10,000 trials for a single pixel is shown in Figure 3. The histogram is roughly Gaussian shaped with a mean of 300 Hz, which was the actual value of the Doppler shift in all of the trials.

As shown in Figure 3, the estimated value of a particular pixel can deviate from its true value. This may produce spurious peaks in the ODT velocity image of the sample. However, the magnitude of the flow direction vector should change smoothly across the image due to the mechanics of uncompressible fluid flow. Thus, we can use the high
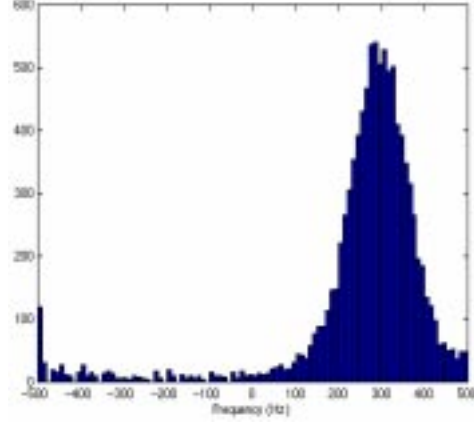

Figure 3: Histogram of $\hat{f}_d$ at one pixel for 10,000 trials. The actual f_d was 300 Hz with $\Delta t = 1$ ms.

spatial correlation between pixels to improve the estimate of the flow vectors. The spatial correlation will eliminate spurious peaks. The algorithm is given in Figure 4.

IV. Performance

From (7) the range of detectable Doppler frequencies for a single pixel is

$$-0.5 < f_d \Delta t \leq 0.5 \qquad (8)$$

This limited frequency range causes a wrap-around effect in the phase, which for the experiment in Figure 3 is –500 Hz. Using one-dimensional phase unwrapping techniques [11] can significantly expand the range in the constraint given by (8). This constraint can be further relaxed with a two-dimensional phase unwrapping technique that uses the gradient in both dimensions.

The frequency resolution Δf_d of the estimate obtained using (7) is

1. For each pixel,
    a. Record $IFD_n(t)$ for a pixel.
    b. Record $IFD_n(t+\Delta t)$ the same pixel.
    c. Find the cross-correlation, $R_T(\tau+\Delta t)$ of $IFD_n(t)$ and $IFD_n(t+\Delta t)$,).
    d. Find location of first peak of $R_T(\tau+\Delta t)$.
    e. Obtain the estimate, $\hat{f}_d$, of the grayscale value of the pixel from (7).
2. Repeat Step 1 for all pixels in the ODT velocity image.
3. Perform 3×3 median filtering on the ODT velocity image.
4. Obtain the estimate by performing 2-D phase unwrapping on the ODT velocity image.

Figure 4: Outline of the proposed algorithm.

$$\Delta f_d = \frac{f_c}{f_s \Delta t} \qquad (9)$$

where f_s is the sampling frequency. The frequency resolution of our algorithm depends on parameters f_c, f_s, and Δt, which are known in practice and preset in simulations; e.g., with f_s=100 MHz, f_c=1 MHz and Δt=1ms, we obtain Δf_d=10 Hz.

The ODT system acquires N_s samples per pixel. The computational cost of the algorithm is dominated by the N_s^2 multiplications in the cross-correlation and the N_s comparisons needed to find the maximum of the cross-correlation. The memory cost for this algorithm is $2N_s$; i.e.,, two sets of N_s samples that are Δt time units apart.

V. Simulation Results

We simulate IFD data that represents a blood vessel of 200 μm radius with its center in the center of the image. The image size is 100×100 pixels, with each pixel being 10×10 μm. All of the results are obtained using data simulated via the physical model in (1) and reconstructed via the AM-FM model in (3). In the simulated data, the carrier frequency is 1 MHz and Δt is 1 ms. The results presented in this section are obtained using the data additive white Gaussian noise yielding an SNR of -3 dB. The algorithm gives high accuracy in the presence of significant noise because the noise does not correlate across shifts in the interference fringe data.

The dashed line in Figures 5 and 6 shows the ideal curve of the blood flow. To reconstruct the vessel in Figure 5, we used 32 bits of precision with 100 MHz sampling rate. At this sampling rate, recording time of 1 μs (the period of f_c) produces 128 samples/pixel. Figure 6 shows the same vessel simulated using 4 bits of precision with 12.5 MHz sampling rate (1 μs ⇔16 samples/pixel). The corresponding data rate would be 1.6 million samples/s for 5 frames/s. At this rate, the algorithm would require 26 million multiply-accumulate operations/s. Hence, the algorithm could be easily implemented in real-time in software.

Figure 7 shows the noise sensitivity of the algorithm. An image of a single blood vessel was simulated many times with varying amounts of noise in the interference fringe data, and the error in the reconstructed image was measured. This graph shows that good results are obtained for even significant amounts of noise. In fact, accurate image reconstruction is possible until the noise power is equal to the signal power.

VI. Conclusions

We have developed a new velocity estimation algorithm for the next generation of ODT systems, which will operate at several frames per second.   Unlike previous ODT algorithms based on the Fourier transform, this nonlinear algorithm can detect a very small Doppler shift (e.g. a 100 Hz shift in a 1 MHz signal) with data from only a tiny fraction of carrier frequency's period (e.g. 0.1% of a period of the carrier frequency). This algorithm, derived from an AM-FM model of the interference fringe data in optical Doppler tomography (ODT) systems, is able to quantify the velocity with remarkable accuracy even with the very short data records in fast ODT systems.   Because of the correlation used in the algorithm, we are able to obtain accurate results even for low SNR (-3 dB). Furthermore, the algorithm is computationally efficient and can be implemented real-time software for the next generation of high-speed optical Doppler tomography systems operating at 1-10 million samples/s.

VII. References

[1] B. S. Rinkevichyus and V. I. Smirnov, "Optical Doppler method for investigating turbulent flow by spectral analysis of a signal," *Sov. J. Quantum Electron.*, vol. 3, no. 2, pp. 146-148, Sep.-Oct. 1973.

[2] J. Wang, T. E. Milner, and J. S. Nelson, "Characterization of fluid flow velocity by optical Doppler tomography," *Optics Letters*, vol. 20, no. 11, pp. 1337-1339, June 1995.

[3] Z. Chen, T. E. Milner, D. Dave, and J. S. Nelson, "Optical Doppler tomographic imaging of fluid flow velocity in highly scattering media," *Optics Letters*, vol. 22, no. 1, pp. 64-66, Jan. 1997.

[4] K. D. Manish, T. G. Van Leeuwen, S. Yazdanfar and J. A. Izatt, "Velocity accuracy enhancement and frame rate limitations in color Doppler optical coherence tomography," *Proc. IEEE Conf. Lasers and Electro-Optics*, San Francisco, CA, May 1998, pp. 125-127.

[5] J. A. Izatt, K. D. Manish, H. Wang, K. Kobayashi and M. V. Sivak, "Optical coherence tomography and microscopy in gastrointestinal tissues," *IEEE J. Selected Topics in Quantum Electronics*, vol. 2, no. 4, pp. 1017-1028, Dec. 1996.

[6] D. L. Jones and T. W. Parks, "A resolution comparison of several time-frequency representations," *IEEE Trans. on Sig. Proc.*, vol. 40, no. 2, pp. 413-420, Feb. 1992.

[7] P. Maragos, J. F. Kaiser, and T. F. Quatieri, "Energy separation in signal modulations with application to speech analysis," *IEEE Trans. on Sig. Proc.*, vol. 41, no. 10, pp. 3024-3051, Oct. 1993.

[8] T. Lindmo, D. J. Smithies, Z. Chen, J. S. Nelson, and T. E. Milner, "Accuracy and noise in Optical Doppler tomography studied by Monte Carlo simulation," *Phys. Med. Bio.*, vol. 43, pp. 3045-3064, Oct. 1998.

[9] J. P. Havlicek, D. S. Harding and A. C. Bovik, "The multicomponent AM-FM image representation," *IEEE Trans. on Image Proc,* vol. 6, no. 5, pp. 1094-1100, June 1996.

[10] J. R. Carson, "Notes on the theory of modulation," *Proc. IRE*, vol. 10, pp. 57-64, 1922.

[11] J. M. Tribolet, "A new phase unwrapping algorithm," *IEEE Trans. on Acoustics, Speech, and Signal Proc.*, vol. 25, no. 2, pp. 170-177, Feb. 1977.
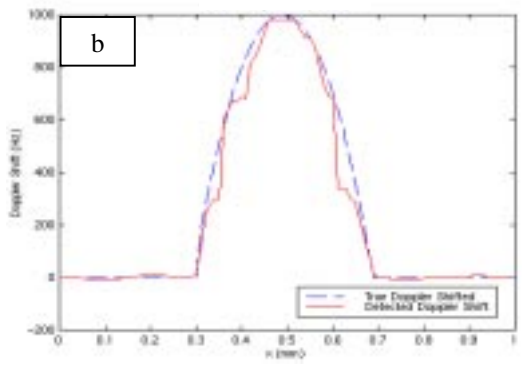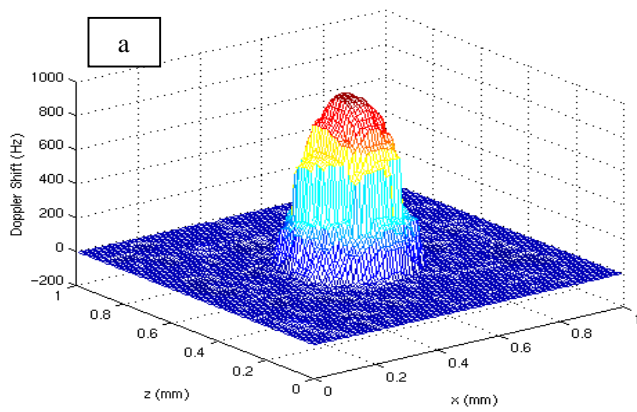
Figure 5: Sampling at 100 MHz using 32 bits/sample
and double-precision floating-point arithmetic:
(a) 3-D reconstruction of the blood flow, and
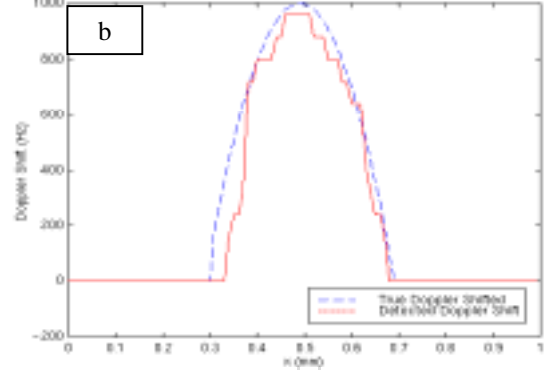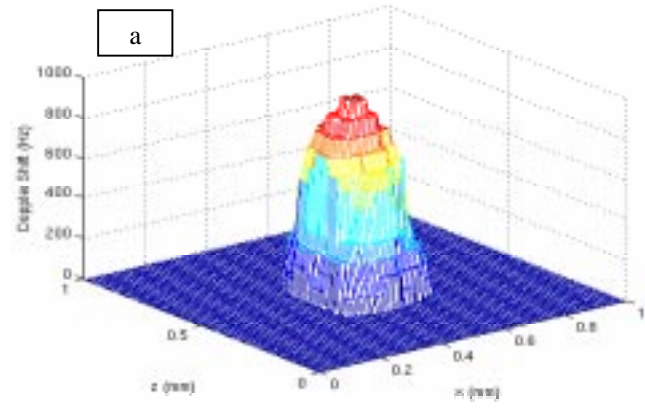(b) axial profile of the estimate

Figure 6: Sampling at 12.5 MHz using 4 bits/sample
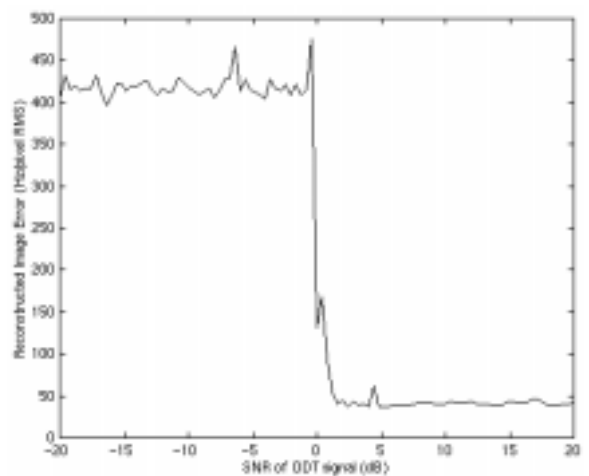and 8-bit arithmetic:
(a) 3-D reconstruction of the blood flow, and
(b) axial profile of the estimate

Figure 7: Noise sensitivity